PHYSICAL REVIEW D **92,** 094030 (2015)

Unveiling the proton spin decomposition at a future electron-ion collider

Elke C. Aschenauer[*]
Physics Department, Brookhaven National Laboratory, Upton, New York 11973, USA

Rodolfo Sassot[†]
Departamento de Física and IFIBA, Facultad de Ciencias Exactas y Naturales, Universidad de Buenos Aires, Ciudad Universitaria, Pabellón 1, (1428) Buenos Aires, Argentina

Marco Stratmann[‡]
Institute for Theoretical Physics, University of Tübingen, Auf der Morgenstelle 14, 72076 Tübingen, Germany
(Received 24 September 2015; published 24 November 2015)

We present a detailed assessment of how well a future electron-ion collider could constrain helicity parton distributions in the nucleon and, therefore, unveil the role of the intrinsic spin of quarks and gluons in the proton's spin budget. Any remaining deficit in this decomposition will provide the best indirect constraint on the contribution due to the total orbital angular momenta of quarks and gluons. Specifically, all our studies are performed in the context of global QCD analyses based on realistic pseudodata and in the light of the most recent data obtained from polarized proton-proton collisions at BNL-RHIC that have provided evidence for a significant gluon polarization in the accessible, albeit limited range of momentum fractions. We also present projections on what can be achieved on the gluon's helicity distribution by the end of BNL-RHIC operations. All estimates of current and projected uncertainties are performed with the robust Lagrange multiplier technique.

DOI: 10.1103/PhysRevD.92.094030 PACS numbers: 13.88.+e, 13.60.Hb, 12.38.Bx

I. INTRODUCTION AND MOTIVATION

The exploration of the nucleon's inner structure and the interactions among its constituents at high energies has been the main protagonist in the quest for a quantitative picture of matter at the most elementary level during the last 50 years. In spite of an impressive wealth of achievements and discoveries, many fundamental questions still remain unanswered today. The origin of the proton spin is a remarkable example for one of these compelling questions still driving the field of nuclear physics. Inspired by the quark parton model, it was originally thought to arise solely from the intrinsic spins of the proton's valence up and down quarks, but this naive view was denied by results from polarized deep inelastic scattering (DIS) experiments in the late 1980s [1] and has remained under experimental and theoretical scrutiny and debate ever since.

The proposed electron-ion collider (EIC) project in the United States [2–4], a versatile machine designed to explore nuclei and polarized light ions at the energy and intensity frontier with the precision of electromagnetic and electroweak probes, will be the next milestone in the quest for gaining a deeper insight into the nucleon's inner workings. Among its remarkable and unprecedented capabilities, an EIC will be able to disclose definitively the role of quark and gluon spins in the proton down to fractions x of a few hundred thousandths of the nucleon's momentum and in a wide range of resolution scales set by virtuality Q of the probing photon in inclusive DIS. Once the intrinsic spin contributions are being tightly constrained, an EIC will deliver early on a first quantitative, though indirect, estimate on the combined orbital angular momenta (OAM) of quarks and gluons needed in the decomposition of the proton spin. Of course, an EIC is also aiming at directly accessing OAM [2–5] which is, however, experimentally much more challenging than inclusive DIS and, hence, will require some years of running and additional theoretical groundwork to bear fruit.

In the phenomenologically very successful framework of perturbative QCD (pQCD) information on how momentum and spin of quarks and gluons are apportioned in the nucleon factorizes in a universal, process-independent way from calculable, short-distance partonic scattering cross sections [6]. In case the incident beams are both longitudinally polarized in the scattering process, helicity parton distributions (PDFs) $\Delta f(x,Q^2)$ are accessible, where f denotes the different (anti)quark flavors q $(\bar{q})$ or the gluon g. For factorization to be a viable approach, the external scale Q characterizing the scattering needs to be large enough, say, above about 1–2 GeV. Upon integration over all momentum fractions x,

[*]elke@bnl.gov
[†]sassot@df.uba.ar
[‡]marco.stratmann@uni-tuebingen.de

$$\Delta f(Q^2) = \int_0^1 dx \Delta f(x, Q^2) \tag{1}$$

the helicity PDFs contain the desired information entering in the decomposition of the proton's spin

$$\frac{1}{2} = \frac{1}{2}\sum_q [\Delta q(Q^2) + \Delta\bar{q}(Q^2)] + \Delta g(Q^2) + \mathcal{L}(Q^2) \tag{2}$$

where $\mathcal{L}(Q^2) = \sum_q [L_q(Q^2) + L_{\bar{q}}(Q^2)] + L_g(Q^2)$ is the total contribution from OAM. The sum of quark and antiquark densities in Eq. (2) can be combined in the quark singlet contribution $\Delta\Sigma(Q^2)$. It should be noted that the apparently simple relation (2) was subject to quite some debate and controversy in recent years. The main problems are that the decomposition (2) is not unique and that the separation of the gluonic total angular momentum into $\Delta g(Q^2)$ and $L_g(Q^2)$ was not thought to be possible in a gauge invariant manner. It is now understood [7] that a particular choice of decomposition is essentially a matter of taste as long as each component can be determined, at least in principle, experimentally or from lattice QCD calculations. Each variant covers complementary aspects of a complex bound-state system such as the nucleon.

In this paper, we are primarily interested in providing the best possible quantitative assessment of the impact a future EIC would have on determinations of the quark singlet and gluon helicity densities and their contributions to the proton spin in Eq. (2). The theoretical framework for our survey is based on an earlier study [8] where we have performed a series of global QCD analyses of helicity PDFs at next-to-leading order (NLO) accuracy including sets of realistic mock EIC data for both polarized DIS and semi-inclusive DIS (SIDIS). These data were generated and properly randomized within one-sigma uncertainties using state-of-the-art spin-dependent PDFs [9,10] based on experimental information from polarized fixed target DIS and SIDIS and proton-proton collisions at BNL-RHIC available at that time.

Since then, many new and important results by the BNL-RHIC experiments [11–16] have been reported, that have changed substantially our perception of the gluon helicity distribution [17]. QCD analyses of the first RHIC spin results [9,10] were dominated by single-inclusive pion production data, obtained at rather low transverse momentum scales p_T, and suggested very little or no gluon polarization in the range $0.05 \lesssim x \lesssim 0.2$ predominantly probed by data, albeit within very large uncertainties. In contrast, the most recent and very precise jet production data [15] from RHIC, taken at larger scales p_T than for pions, provided for the first time clear evidence for a sizable gluon polarization [17]. Very similar results have been reported in an independent global QCD analysis in Ref. [18] based on neural networks, which largely avoids assumptions about the functional form of PDFs inherent to more traditional fitting methods [9,10,17]. It is important to notice that both sets of recent inclusive measurements at RHIC which are highly sensitive to the gluon helicity PDF, jets [15] and pions [16], are fully consistent with each other if one properly takes into account the different scales p_T and ranges of momentum fractions x probed by the respective data. This is automatically guaranteed and achieved in the framework of a global QCD analysis at NLO accuracy based on exact, unabridged NLO expressions for the underlying spin-dependent pp cross sections [19,20]. The neural network analysis in [18] does not make use of any pion production data yet, which explains their larger uncertainties on Δg in the relevant kinematic region as compared to the global fit in [17]; see, e.g., Ref. [21] for a comparison of the two results.

In light of these new results from RHIC pertaining to the relevance of gluons in the nucleon's spin decomposition it is of critical importance to reexamine our previous impact study [8] to update the case for a future polarized DIS program at an EIC. Apart from including the latest RHIC spin data we will also refine and expand our study in many other important aspects. To establish a meaningful baseline for estimating the impact of future EIC DIS data, we first present projections of what will likely be the final word from the RHIC spin program with respect to $\Delta g(x, Q^2)$ and its integral $\Delta g(Q^2)$. To this end, we add realistic projections for yet to be published inclusive jet and pion data from polarized pp collisions at 200 and 510 GeV [22] to the global QCD analysis framework of Ref. [17]. First, preliminary results [23] for these measurements are fully consistent with the most recent global fits of helicity PDFs [17,18]. Next, we update and include the sets of mock polarized DIS data to reflect the latest collision energies envisioned for the eRHIC option of an EIC [4]. Throughout, we pay special attention to properly estimate the impact of the different data sets in the various regions of parton momentum fraction x.

Once we have completed our extensive studies of the prospects for the gluon helicity density $\Delta g(x, Q^2)$ and its integral $\Delta g(Q^2)$ from both the RHIC spin program and a future EIC, we will consider the quark spin contribution $\Delta\Sigma(x, Q^2)$ summed over all flavors. Finally, we will examine what can be gleaned from these two projections for the total parton OAM contribution $\mathcal{L}(Q^2)$ when combined with the spin decomposition (2).

As a technical improvement, we introduce in all our impact studies a more robust treatment of uncertainties. Specifically, we now estimate uncertainties with the Lagrange multiplier technique [24] considering dynamical tolerances corresponding to the 90% confidence level (C.L.) [17] as it is customary in most current fits of unpolarized parton densities [25], rather than adopting some *ad hoc* fixed $\Delta\chi^2$ criterion as in our previous analyses [8–10]. This new procedure takes into account more precisely the role of the different observables in

constraining parton densities at different kinematic regions in x and Q^2.

We have to postpone a new detailed study of the flavor separated helicity quark distributions $\Delta f(x, Q^2)$ as a proper global QCD analysis of projected polarized SIDIS data with identified pions and kaons for an EIC critically depends on having available a reliable set of parton-to-hadron fragmentation functions (FFs) and their uncertainties. At this point, only pion FFs have been updated recently [26] and kaon FFs, important for determining the strangeness polarization, are still a work in progress [27]. Also, RHIC spin data, this time for the longitudinal single spin asymmetry of $W^{\pm}$ bosons [22], are expected to play a significant role in establishing a meaningful baseline for impact studies of flavor separated $\Delta f(x, Q^2)$ from SIDIS measurements at an EIC. However, the final data sets from RHIC are not yet available. Finally, we note that for this study we focus in general on the so far unmeasured region of small momentum fractions and, correspondingly, low-to-medium values of Q^2 at an EIC. The prospects of DIS measurements with an EIC in the region where $Q \simeq M_W$ was studied in some detail in Ref. [28] based on NLO expressions for the charged current DIS given, for instance, in [29].

In the remainder of the paper, we first briefly discuss the sets of pseudodata generated to study the impact of both polarized DIS at an EIC and upcoming RHIC pp data in determinations of the gluon and quark singlet helicity distribution and their respective integrals. In Secs. III and IV we present the results of our global QCD analyses at NLO accuracy based on including these sets of data one by one. First, we focus on what can be expected for $\Delta g(x, Q^2)$ by the end of the RHIC spin program and, next, we include also the mock EIC data. Our main results are best presented in terms of "running x-integrals" for Δg (in Sec. III), $\Delta\Sigma$, and the difference between $1/2$ and $\frac{1}{2}\Delta\Sigma + \Delta g$ (in Sec. IV), that represents roughly how much room is left for OAM to saturate the spin sum rule. Finally, we summarize our results and present our conclusions.

II. SIMULATED DATA FOR POLARIZED DIS AT AN EIC

Inclusive DIS with longitudinally polarized leptons and nucleons can be expressed by the structure function $g_1(x, Q^2)$. For energy scales Q well below the mass of the electroweak gauge bosons $W^{\pm}$ and Z, the scattering is mediated by the exchange of a virtual photon and both kinematic variables x and Q^2 can be straightforwardly reconstructed from measuring the energy and angle of the deflected lepton.

Sensitivity to the gluon helicity distribution $\Delta g(x, Q^2)$ in DIS is manifold: directly, through higher order QCD corrections to g_1, which are subleading compared to the dominant quark contribution and, hence, small and difficult to utilize in an analysis, or, indirectly, through scaling violations, that is, variations of the structure function $g_1(x, Q^2)$ with scale Q for *fixed* values of x. The smaller x the more pronounced are the scaling violations, which are usually expressed as the logarithmic derivative of the DIS structure function, i.e., $dg_1(x, Q^2)/d\ln(Q^2)$. It should be noted that corresponding results for unpolarized DIS from the DESY-HERA experiments [30] are utilized in all current extractions of helicity-averaged PDFs and provide by far the best constraint on the gluon density below about $x \simeq 0.05$ [25]. Through evolution, $\Delta g(x, Q^2)$ is also correlated with the quark singlet helicity distribution, at small x mainly to the sea component, which itself is very poorly constrained below the range of existing polarized DIS data covering $x \gtrsim 0.004$ for $Q^2 > 1$ GeV^2 [1,31]. As we shall see below, this also leads to a significant uncertainty in current estimates of $g_1(x, Q^2)$ and, hence, in the quark singlet $\Delta\Sigma(Q^2)$ entering (2), which only an EIC can finally resolve. At variance with unpolarized PDFs, where the scale evolution at small x is driven by gluons, quark and gluon helicity PDFs are equally important as they exhibit a similar, less singular $x \to 0$ behavior in all evolution kernels [32]. The different evolution of helicity and helicity-averaged distributions also leads to a strong suppression of gluon and quark polarizations as $x \to 0$ and, consequently, of all spin asymmetries in that kinematic region.

Thus, in order to get an accurate picture of the gluon and quark helicity densities and, in particular, their x-integrals (1) at an EIC it is not only crucial to have good precision in a wide range of parton momentum fractions x to reduce extrapolation uncertainties from the currently unmeasured x region in DIS, but also to cover for any given x the largest possible range in the photon virtuality Q^2 to determine Δg from scaling violations. The requirement of being able to reach x values well below what has been achieved so far [1,31] for virtualities Q^2 safely in the DIS regime, say, above at least 1 GeV^2, clearly calls for the largest conceivable center-of-mass system (c.m.s.) energies $\sqrt{s}$ at a future ep collider in order to make any significant impact. Furthermore, at small x the reach in Q^2 to study scaling violations, which are only logarithmic in energy, is kinematically limited to $Q^2 = sxy$ where y is the fractional energy of the virtual photon. y is constrained by the increasing depolarization of the virtual photon from below, which should not exceed about 90%, and, from above, by the energy of the scattered lepton, which should be not too low to be still reliably measurable in the detector. In practice, $0.01 \lesssim y \lesssim 0.95$ appears to be a reasonable choice as the DESY-HERA collider experiments even used the range $0.005 \lesssim y \lesssim 0.95$ for parts of their physics program.

In our previous study [8], we adopted c.m.s. energies from $\sqrt{s} \simeq 45$ GeV to 71 GeV corresponding to an electron beam energy of 5 GeV for the BNL eRHIC design of an initial version of an EIC at that time. As a potential

TABLE I. Combinations of electron and proton energies of the current eRHIC design [4] as used in our analyses, the corresponding c.m.s. energies, and the range in x accessible for $Q^2 = 1$ GeV^2 and assuming $0.01 < y < 0.95$.

$E_e \times E_p$ (GeV)	$\sqrt{s}$ (GeV)	$x_{\min}$ for $y = 0.95$	$x_{\max}$ for $y = 0.01$
15×100	77.5	1.8×10^{-4}	1.7×10^{-2}
15×250	122.7	7.0×10^{-5}	6.7×10^{-3}
20×250	141.4	5.3×10^{-5}	5.0×10^{-3}

later upgrade we also considered $E_e = 20$ GeV leading to a maximum $\sqrt{s} = 141.4$ GeV. The latest eRHIC design evolved considerably and now has a default electron beam energy of about 15 GeV but is also capable to run with both lower and higher lepton energies at similar luminosities [4] from day 1. When combined with the existing RHIC proton beam of up to $E_p = 250$ GeV this setup not only extends the reach towards small x by almost two decades compared to what is known today but also makes the detection of the scattered electron at large y much easier than for a 5 GeV electron beam. Table I summarizes the three different c.m.s. energies we are going to consider in this study along with the accessible range in x, $[x_{\min}, x_{\max}]$, for $Q^2 = 1$ GeV^2, assuming the same standard DIS cuts as in our previous analysis [8]: $Q^2 > 1$ GeV^2, $W^2 > 10$ GeV^2, and $0.01 \leq y \leq 0.95$. As can be seen, the improvements in the kinematic range for both x and Q^2 from $\sqrt{s} = 122.7$ to 141.4 GeV corresponding to $E_e = 15$ GeV and 20 GeV, respectively, are not too significant.

In order to generate the mock polarized DIS data for the energies shown in Table I, we proceed very much in the same way as was detailed in Ref. [8]. The statistical accuracy for each of the generated data sets is scaled to correspond to a very modest accumulated integrated luminosity of 10 fb^{-1}, equivalent to at most a few months of operations for the anticipated luminosities for eRHIC [4] and 50% efficiency in the data taking. We assume 70% polarization for both the electron and the proton beam. Each of the three new sets adds about 70 points to the existing suite of fixed target DIS spin asymmetry data, distributed logarithmically in 4 (5) bins per decade in Q^2 (x). As in Ref. [8], the actual data used in our global analyses below are not the generated ones but theoretical estimates of the spin asymmetry at NLO accuracy based on the latest DSSV helicity densities [17], reflecting the same relative statistical accuracy in each x, Q^2 bin as the Monte Carlo data, and having their central values randomized within one-sigma uncertainties.

In any case, the DIS measurements at an EIC will be mainly limited by systematical errors due to detector performance, beam polarization and luminosity measurements, and the unfolding of QED radiative corrections, which we all assume to be controlled to a percent level accuracy. This will be necessary for achieving meaningful constraints on the helicity PDFs as we have already demonstrated in our previous analysis; see, e.g., Fig. 6 in Ref. [8]. We note that the typical size of the DIS spin asymmetries at the lowest values of x can be as small as a few times 10^{-4}. Such measurements are already routinely performed at RHIC in case of double spin asymmetries for single-inclusive pion production [16] at transverse momenta p_T of a few GeV.

To illustrate the main idea of the planned measurements in polarized DIS, the enhanced kinematic coverage at an EIC, and the current uncertainties which prevent us from having a clear picture of how quarks and gluons generate the proton's spin, we start with presenting the scale dependence of the gluon helicity density. Figure 1 shows the shape of $\Delta g(x, Q^2)$ as extracted from the latest global QCD analysis to all presently available data in DIS, SIDIS, and pp collisions [17] (henceforth denoted as "DSSV 2014 best fit"). The plot illustrates how the QCD scale evolution quickly broadens the x-shape of $\Delta g(x, Q^2)$ with increasing Q^2, which is initially largely concentrated at rather high momentum fractions x at a scale of $Q^2 = 1$ GeV^2, and moves its peak rapidly towards smaller values of x. The main constraint on $\Delta g(x, Q^2)$ so far is derived from the latest RHIC inclusive jet and π^0 [15,16] which span, as is indicated in Fig. 1, only a rather limited range in both x

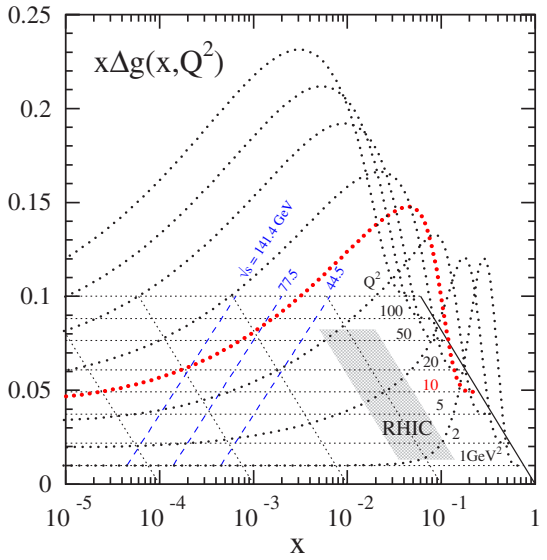

FIG. 1 (color online). QCD scale evolution of the optimum DSSV 2014 gluon helicity distribution [17] as a function of the momentum fraction x for various values of Q^2 (dotted curves). The dashed lines delineate the minimal x accessible at an EIC in the $x - Q^2$ plane for various c.m.s. energies and $y = 0.95$. The line for $\sqrt{s} = 44.5$ GeV corresponds to an energy considered in our previous paper [8] utilizing only a 5 GeV electron beam at eRHIC. The shaded area labeled "RHIC" shows approximately the region where $\Delta g(x, Q^2)$ is constrained best by published RHIC pp data [15,16].

and Q^2, the latter being approximately determined by the measured range of p_T (a few GeV to about 20–30 GeV). Clearly, nothing is known about the low momentum fraction tail of $\Delta g(x, Q^2)$ beyond the part of it generated radiatively by evolution from lower Q^2 and larger x. In the next section, we will elaborate in detail on the present uncertainties for $\Delta g(x, Q^2)$, which appear to very substantial, in particular, in the unmeasured small x region. In general, spin asymmetries sensitive to small x are very difficult to seize experimentally as the unpolarized gluon density rises sharply as $x \to 0$, leading to a more and more suppressed gluon polarization $\Delta g/g$, and likewise for sea quark polarizations.

To emphasize the importance of running an EIC at the largest possible c.m.s. energy, we also overlay in Fig. 1 the kinematic lower limits in x and Q^2 for various values of $\sqrt{s}$ and assuming $y \leq 0.95$; see Table I. The line for $\sqrt{s} = 44.5$ GeV corresponds to the no longer considered lowest c.m.s. energy of our previous study [8]; as was mentioned above, the new design for eRHIC allows us to cover significantly lower values of x from the very beginning of operations.

Figure 2 illustrates our updated simulated data sets for inclusive polarized DIS at an EIC for the three different choices of c.m.s. energies listed in Table I. The solid lines reflect the expectations from the best fit of DSSV 2014 [17] by extrapolating their results outside the experimentally constrained x and Q^2 range. The shaded bands illustrate the uncertainty estimates corresponding to the 90% C.L. variations of $\Delta g(x, Q^2)$ given in Ref. [17], which cover a very significant spread below about $x \simeq 0.01$; see also Fig. 1 in Ref. [17]. The error bars for the EIC pseudodata were determined as described above and in Ref. [8] and reflect the expected statistical accuracy for a modest integrated luminosity of 10 fb^{-1}, 70% beam polarization, and 50% efficiency in the data taking. We recall that all currently available polarized DIS data cover only the lower left corner in Fig. 2 with the smallest x, $x \simeq 3.6 \times 10^{-3}$, being reached by the recent COMPASS data [31] for $Q^2 \simeq 1$ GeV^2. As can be seen, in the kinematic region already covered well by present fixed target data, $x \gtrsim 0.01$, the remaining uncertainties in $g_1(x, Q^2)$ are very small. For smaller x, the precision of the projected EIC data is significantly better than current uncertainties and these measurements will be the decisive factor in future global fits as we shall illustrate in the next section.

One notices the rather modest scaling violations $dg_1(x, Q^2)/d\ln Q^2$ for the optimum DSSV 2014 fit throughout the entire x and Q^2 range shown in Fig. 2, in particular, if compared to similar plots for the unpolarized DIS structure functions [30]. On the one hand, this is due to the less singular scale evolution for helicity PDFs at small x, and, on the other hand, there is also a potential delicate cancellation with the quark helicity PDFs, which,

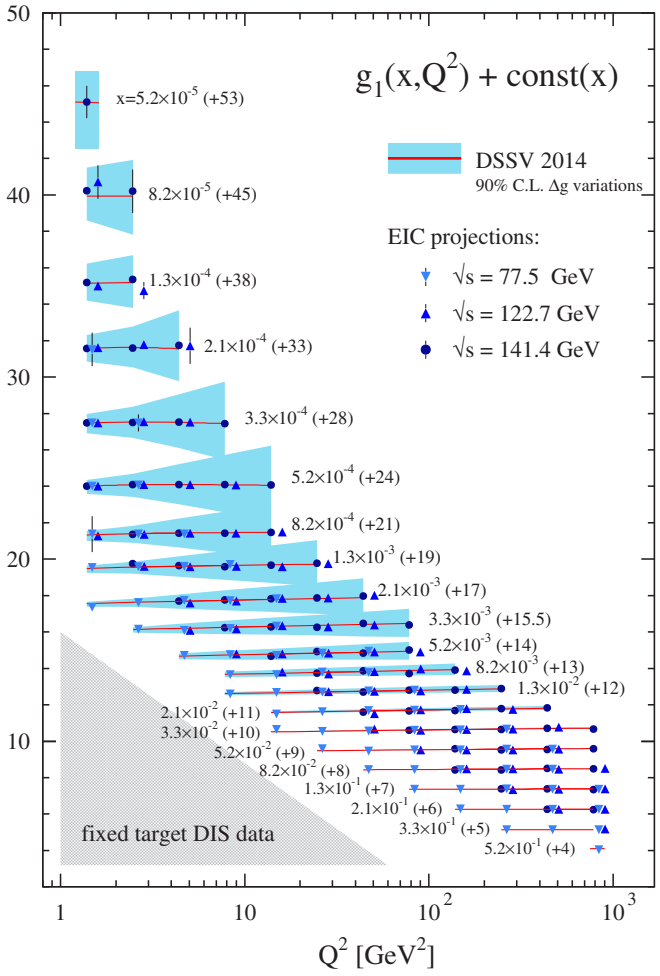

FIG. 2 (color online). Projected EIC data for the structure function $g_1(x, Q^2)$ for the different combinations of electron and proton energies in Table I. Constants are added to g_1 to separate the different x bins and multiple data points in the same (x, Q^2) bin are slightly displaced horizontally. The solid lines are obtained for the optimum DSSV fit of 2014 [17] and the shaded bands illustrate the 90% C.L. uncertainties due to variations in the *gluon helicity density*. The shaded region in the lower left corner illustrates the (x, Q^2) region covered by present fixed target data.

as Δg itself, are not bound to be positive definite and, in addition, can have different signs for different flavors. Therefore, alternative fits, like those for Δg shown in Fig. 1, will all exhibit somewhat different patterns of scaling violations than the optimum DSSV 2014 fit.

As we shall see next, our current ignorance of the small x behavior of helicity quark densities also imposes a significant uncertainty on expectations for $g_1(x, Q^2)$ in the EIC regime. In Fig. 3 we present the DIS structure function $g_1(x, Q^2)$ (solid line) and 90% C.L. estimates of its uncertainties (dotted lines) as a function of the momentum fraction x at $Q^2 = 10$ GeV^2. Unlike in Fig. 2, the alternative fits at 90% C.L. now include *combined* variations of quark and gluon helicity PDFs away from the DSSV 2014

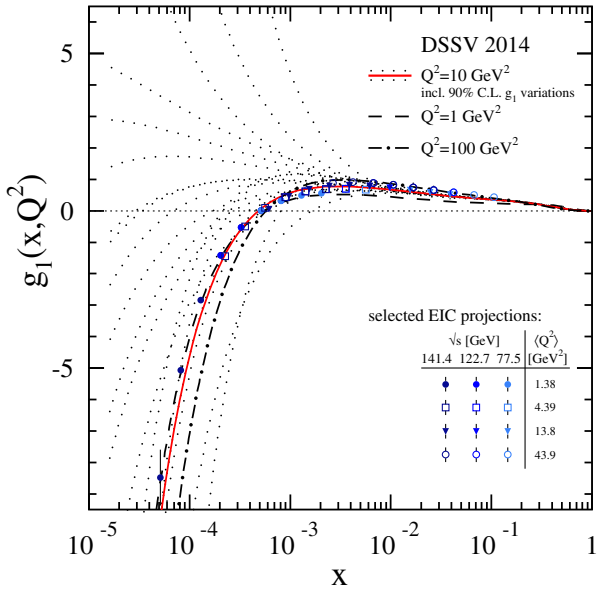

FIG. 3 (color online). The polarized DIS structure function $g_1(x, Q^2)$ at $Q^2 = 10$ GeV^2 as a function of x computed with the optimum DSSV 2014 helicity PDFs [17] (solid line). The dotted curves represent alternative fits within 90% C.L. uncertainties. The dashed and dot-dashed lines show the effects of the scale evolution from $Q^2 = 1$ GeV^2 to 100 GeV^2. The points illustrate typical uncertainties and the kinematic reach of projected EIC data for the three different c.m.s. energies listed in Table I.

best fit [17] which lead to uncertainties at least twice as large as for the variations just based on Δg shown in Fig. 2. We note that throughout our paper the allowed ranges of variations at 90% C.L. are determined for each of the shown results by the robust Lagrange multiplier technique and dynamic tolerances for the appropriate increase in the χ^2 of the fit similar to what is done in most of the recent PDF fits [25].

To illustrate once again the accuracy of future measurements at an EIC, we also show here a few representative projected data points taken from Fig. 2 in the relevant Q^2 regime around 10 GeV^2 for the three different c.m.s. energies we consider. Clearly, measurements of $g_1(x, Q^2)$ at small x will dramatically reduce the uncertainties in the quark helicity PDFs and, indirectly, through the coupled QCD scale evolution of quarks and gluons also in $\Delta g(x, Q^2)$. At any given x, scaling violations for $g_1(x, Q^2)$ will further constrain $\Delta g(x, Q^2)$. As was already shown in Fig. 2, they are numerically not very pronounced for the optimum DSSV 2014 fit, which can be also inferred from Fig. 3, where we show $g_1(x, Q^2)$ at $Q^2 = 1$ and 100 GeV^2 in addition to our default scale of 10 GeV^2. However, each of the alternative fits exhibits a somewhat different Q^2 dependence driven by the uncertainties in the x-shapes of the quark and gluon densities. For $x \gtrsim 0.01$, the scale dependence of $g_1(x, Q^2)$ in the range from $Q^2 = 1$ to 100 GeV^2 is typically larger than the uncertainty on $g_1(x, Q^2)$ from present data.

III. PRESENT STATUS OF Δg AND IMPACT OF PROJECTED RHIC AND EIC DATA

Before addressing the question of how precisely an EIC will constrain the total gluon and quark polarizations in the spin decomposition (2) and, indirectly, also the total OAM $\mathcal{L}$, it is important to first make a precise assessment of how well these quantities are expected to be known by the end of the current experimental programs, in particular, RHIC spin. This will set the best possible baseline to judge the impact that a future EIC could have in the field of QCD spin physics.

Different indicators and measures can be adopted to quantify how well the gluon helicity density and the resulting contribution $\Delta g(Q^2)$ to the proton's spin are constrained by data. The standard way to study uncertainties as a function of the parton's momentum fraction x at a given Q^2 in a global QCD fit to all available data is certainly the most obvious possibility; however, it neither provides an immediate idea of the accuracy for the phenomenologically interesting x-integral (1) that is the focus of our study, nor does it indicate the relevance of the different regions in x probed by the different experiments used in the fit.

Instead, we choose to present most of our results in terms of the "running integral" of, for instance, the gluon helicity density, defined analogously to Eq. (1) as

$$\Delta g(Q^2, x_{\min}) \equiv \int_{x_{\min}}^{1} dx \Delta g(x, Q^2), \tag{3}$$

which represents the share of the proton spin (2) from gluons as a function of the lower integration limit $x_{\min}$. Its uncertainty takes into account the nontrivial correlations between the different regions of x contributing to (3). By varying $x_{\min}$ in (3), one can explore how low in x (or, alternatively, how high in $\sqrt{s}$) one likely needs to go with future experiments to reduce $x \to 0$ extrapolation uncertainties to a level small enough to make meaningful statements about how gluons and quarks in the proton make up its spin. To study the important question of the convergence of (3) with $x_{\min}$ in more detail, we will also compute the contributions to (3) from different bins $[x_{\min}, x_{\max}]$ in x in case of Δg.

Throughout our analyses, we adopt exactly the same conventions as in the latest DSSV 2014 global fit [17], in particular, the same functional form to describe the helicity parton densities at the initial scale $Q_0 = 1$ GeV. The required high flexibility of this parametrization is guaranteed by a series of additional tests that are customarily performed in global analyses to avoid as much as possible any potential bias from the chosen functional form [9,10,17]. To this end, we have systematically varied the number of free fit parameters to ensure that no significant improvements in the quality of our fits or changes in the presented estimates of uncertainties are found when

comparing to actual or pseudodata sets. The specific details of these exercises give no extra information, other than that there are no noticeable changes in our results, and, hence, for the sake of brevity, we choose not to present them in the following. Of course, it would be nice to have an independent cross-check of our results in the future, preferably, with the largely bias-free neural network approach mentioned in the Introduction. In principle, new data sets can be easily accommodated in this framework by properly reweighing the existing set of Monte Carlo PDF replicas [18]. However, reweighing cannot cope with the large amount of projected data sets from both RHIC and an EIC that we will study in the following. The fact that the latest neural network analysis [18] does not contain any of the existing inclusive pion production data from RHIC, which were found to have quite some impact in the DSSV 2014 fit [17] at the lower end of the x range accessible at RHIC, is an additional complication. We note that projected EIC data were shown to have a significant impact on the helicity gluon density in an earlier study based on the neural network approach [33] when added to an analysis based only on existing fixed-target DIS data, i.e., without using the information available from the RHIC spin program. Hopefully, this kind of analysis will be updated in the near future based on a similar set of actual and projected data as is presented here.

To estimate the impact of past, current, and future data sets on Δg and $\Delta\Sigma$ we proceed in steps. To this end, we will present uncertainty estimates for various running integrals by including different data sets one by one into our global analysis framework. As we have mentioned already, to demonstrate the impact an EIC will have on Δg in the future, we should take into account the experimental information that is expected to become available soon from the RHIC spin program. Essentially, the RHIC running focusing on longitudinally polarized double-spin asymmetries has concluded in 2015, and several high impact data sets are forthcoming, some of which have been presented in preliminary form at conferences recently [23]. Since the expected statistical accuracy of these measurements is already known, we can proceed by generating mock RHIC pp data with the proper uncertainties to estimate their impact on helicity PDFs, in particular, the gluon.

Since extending the reach towards smaller values of x is the most important asset to arrive at a more solid estimate for the integral $\Delta g(Q^2)$, we only focus on upcoming RHIC measurements which have the best potential to do so, i.e., inclusive jet and neutral pion data from STAR and PHENIX, respectively, taken at the highest c.m.s. energy of 510 GeV for pp collisions at RHIC. In particular, spin asymmetries at forward rapidities will allow one to probe x values down to about a few times 10^{-3}, significantly below the currently covered range in x indicated in Fig. 1. More specifically, our projections comprise double spin asymmetries for

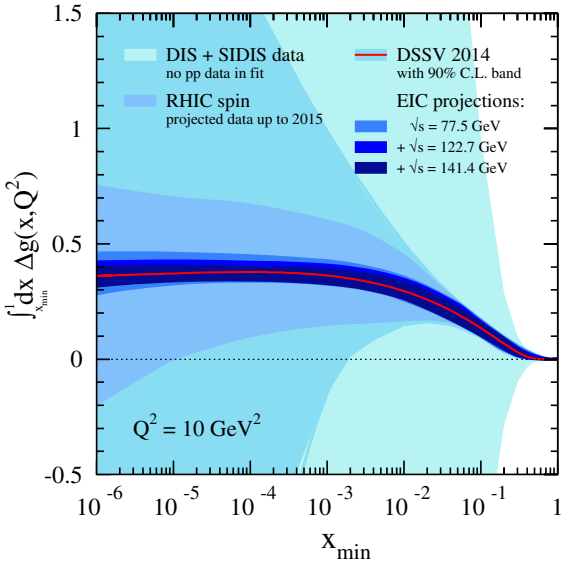

FIG. 4 (color online). The running integral of the gluon helicity distribution at $Q^2 = 10$ GeV^2 as a function of $x_{\min}$ according to the DSSV 2014 analysis [17] (solid line) and 90% C.L. uncertainty estimates (shaded bands) based on global QCD fits utilizing different sets of existing and projected pp and EIC data (see text).

(i) inclusive jet data at midrapidity,
(ii) inclusive π^0 data at midrapidity, and
(iii) inclusive π^0 data at forward rapidities .

In Fig. 4 we show the running integral (3) of the gluon helicity distribution at $Q^2 = 10$ GeV^2 down to $x_{\min} = 10^{-6}$. Concentrating first on the optimum DSSV 2014 fit (solid line), one notices that the integral saturates and reaches more than 90% of its total value $\Delta g(Q^2 = 10\ \text{GeV}^2)$ already for $x_{\min} \simeq 10^{-3}$, suggesting that most of the gluon spin contribution to the sum (2) stems from momentum fractions above 10^{-3}. This is in line with common expectations [34] that $\Delta g(x, Q^2)$ behaves like $xg(x, Q^2)$ at sufficiently small values of x. The preferred value for the gluon spin contribution at $Q^2 = 10$ GeV^2 in the DSSV 2014 analysis [17] turns out to be rather large, about 0.37, corresponding to roughly 70% of the proton spin. However, neither the preferred small x behavior nor the large value for $\Delta g(Q^2 = 10\ \text{GeV}^2)$ is based on actual experimental constraints in the QCD analysis as is illustrated by the various uncertainty bands shown in Fig. 4. Here and in the following, all uncertainty bands correspond to 90% C.L. estimates.

The outermost light shaded bands in Fig. 4 represent a global QCD fit based solely on existing polarized fixed target DIS and SIDIS data [1]. One can safely conclude that these data do not constrain the gluon helicity density or its running integral by any means. The importance of the current RHIC polarized pp data for inclusive jet and π^0 production [11–16] in constraining $\Delta g(x, Q^2)$ down to

about $x \simeq 0.01$ is exemplified by the second level of shaded bands. Still, for smaller values of $x_{\min}$ possible variations in the truncated integral away from its best fit value quickly become very large due to the flexible functional form adopted in the DSSV framework. At least, the analysis suggests at 90% C.L. that the truncated integral (3) stays positive down to $x_{\min} \simeq 2 \times 10^{-3}$, but nothing can be concluded about the full integral $\Delta g(Q^2)$, not even its sign. These uncertainties correspond to those obtained in the DSSV 2014 global analysis [17] and represent our current knowledge.

Next, we include the projections for the upcoming RHIC pp data as listed above into the global analysis framework to estimate what can be expected to be known about $\Delta g(Q^2)$ by the end of RHIC operations and before an EIC will turn on. Any impact of a future EIC needs to be judged with respect to this baseline. As can be seen, RHIC can be expected to further constrain the gluon helicity distribution and, in particular, its running integral, mainly by ruling out very extreme, positive or negative, variations at small momentum fractions. This will be mainly achieved by measurements at forward rapidities. Even though these data will have no sensitivity below $x \simeq 10^{-3}$, they considerably limit possible variations within the given very flexible functional form of the DSSV analysis. Together with the decreasing weight of the region of very small x in the running integral (3), the error on the integral down to $x_{\min} \simeq 10^{-6}$ is significantly reduced but it still covers about twice the proton spin of $1/2$ and ranges roughly from -0.25 to 0.75.

We are now in a position to focus on the impact of the generated EIC data shown in Fig. 2. To this end, we successively add the three sets of mock data given in Table I starting from the lowest c.m.s. energy of $\sqrt{s} = 77.5$ GeV to the global set of data, including the RHIC projections just discussed. The series of the innermost dark shaded bands in Fig. 4 represents the corresponding uncertainty estimates. The results clearly show that for momentum fractions $x \gtrsim 0.05$, DIS, SIDIS, and RHIC data, as included in the DSSV 2014 analysis [17], constrain the running integral adequately well whereas an EIC adds very little new here, apart from a crucial, independent check of what has been learned so far in that particular kinematic region.

The constraining power of an EIC starts to become increasingly noticeable below $x \simeq 0.01$. Already at around $x_{\min} \simeq 10^{-3}$, EIC DIS data are expected to reduce the uncertainties by approximately a factor of 8 as compared to the DSSV 2014 estimate, and by a factor of 4 relative to the projections based on future RHIC data. Below $x_{\min} \simeq 10^{-3}$, EIC data will constrain the flexible functional form for $\Delta g(x, Q^2)$ adopted both in the DSSV and our analyses in such a way that uncertainties in the running integral remain constant, excluding extreme variations in the gluon helicity density at small x still allowed in fits based solely on current or projected RHIC data.

Using only EIC data with the lowest c.m.s. energy considered in our analysis would lead to a determination of the gluon spin contribution to (2) to within a relative uncertainty of about 25%. Including data at higher $\sqrt{s}$ would further reduce relative uncertainties in $\Delta g(Q^2)$ to a level of about 10%. We stress again, that for all our studies, the EIC mock data are generated and randomized around the small x extrapolation of the DSSV 2014 best fit (solid line in Fig. 4). An EIC would be able to either verify if gluons indeed contribute only very little to the running integral below $x_{\min} \simeq 10^{-3}$, as is usually expected [34], or to determine decisively if they exhibit any different behavior at small x. In the latter case, depending on at which $x_{\min}$ the running integral starts to saturate to its full value, DIS data at the largest possible c.m.s. energy are potentially most relevant to have.

The relevance that different regions in x have in the running integral shown above is analyzed more closely in Figs. 5 and 6. Figure 5 illustrates the comparative impact of gluons to the spin sum (2) in different bins of x, four per decade, and the corresponding uncertainties down to 10^{-3} expected to be accessible with forthcoming RHIC pp data. The solid (dashed) lines in each bin are the estimates computed with the DSSV 2014 [17] and 2008 [9] fits, respectively. The dotted line gives the cumulative contribution to the running integral (3) as was shown in Fig. 4. The arrow indicates the value of the full integral $\Delta g(Q^2 = 10\ \text{GeV}^2)$. In addition, 90% C.L. uncertainty estimates are shown for each individual bin. We notice

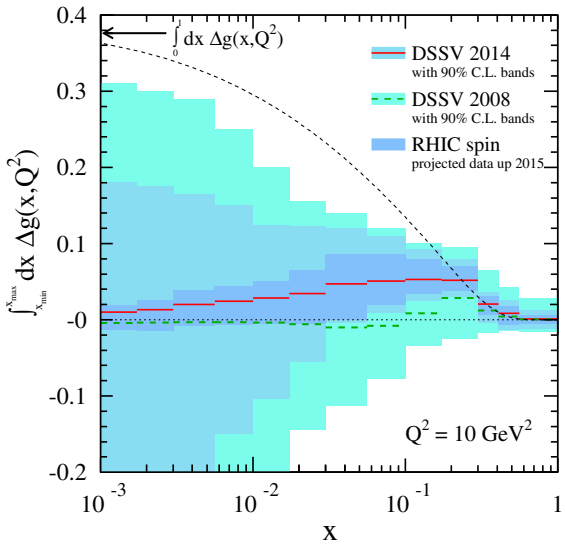

FIG. 5 (color online). Contributions to $\Delta g(Q^2)$ in (2) at $Q^2 = 10\ \text{GeV}^2$ from different x intervals (see text). The solid and dashed lines represent the results from the DSSV 2014 [17] and 2008 [9,10] best fits, respectively, which mainly differ by the latest RHIC pp data [15,16]. The various shaded bands reflect 90% C.L. uncertainty estimates for both fits and the impact of forthcoming RHIC data. The dotted line indicates the cumulative contribution to $\Delta g(Q^2)$ for DSSV 2014.

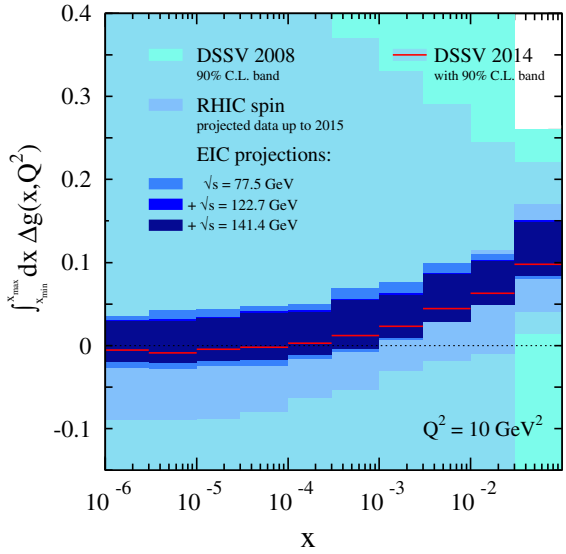

FIG. 6 (color online). As in Fig. 5 but now focusing on the small x extrapolation and the impact of the projected polarized DIS data sets shown in Fig. 2 on the 90% C.L. uncertainty estimates.

that the partial contributions of each bin in x to the running integral (3) and the corresponding variations are very strongly correlated to those of the neighboring bins. As a consequence, the sum of the individual uncertainties from each bin can exceed the uncertainty of the running integral shown in Fig. 4. Nevertheless, they correctly reflect the relative impact of the different bins in x. In each bin the uncertainties reflect the synergy of all the different data sets included in the global analysis.

The outermost shaded bands in Fig. 5 correspond to the DSSV 2008 analysis, the middle ones to the most recent 2014 fit. The optimum gluon helicity distribution in the 2008 fit had an almost vanishing contribution to the proton spin sum rule [9] and was characterized by a node in the x region probed by available RHIC data at that time. These features can be easily gathered also from Fig. 5. The current 2014 best fit based on the latest RHIC pp data has a much larger and positive $\Delta g(x, Q^2)$; cf. Fig. 1. As can be inferred from Fig. 5, only the x region probed by the pp data contributes significantly to the integral. As is expected from Fig. 4, uncertainties for the old DSSV 2008 analysis are significantly larger than those for the 2014 fit in all bins of x, but both fits cannot constrain contributions to the running integral below $x \lesssim 0.01$ in any meaningful way. Here, uncertainties sharply increase with decreasing x. The innermost, dark shaded uncertainty bands demonstrate the constraining power of the projected RHIC data which now, unlike for the previous results, exhibit decreasing uncertainties with smaller values of x.

In Fig. 6 we extend the x range down to 10^{-6} and include bin-by-bin uncertainty estimates based on the three sets of projected DIS data at an EIC. Compared to Fig. 5, we now use only two bins per decade in x. Below $x \sim 10^{-3}$ the contributions to the integral in each bin remain small for the DSSV 2014 best fit (solid line), fluctuating around zero, but the corresponding uncertainties continue to increase for both the 2008 and 2014 fits. Uncertainty estimates including also the projected RHIC data only slightly increase towards smaller x reflecting the improvements in the running integral already observed in Fig. 4. The constraining power of the EIC DIS data is very significant in the entire x range and appears to be roughly a constant factor of 2–3 with respect to the bin-by-bin estimates including the projected RHIC data. This is somewhat less than what was obtained for the running integral at low x_{min}, suggesting that scaling violations are more powerful when considered over an extended range of momentum fractions rather than in a small bin in x. In the latter case many fewer data points are actually providing a strong constraint on allowed variations in any given bin. Another important factor to consider is the mentioned sizable bin-by-bin correlations. Similarly, the impact of including more DIS sets at different c.m.s. energies is reduced for the bin-by-bin studies as compared to the running integral shown in Fig. 4.

IV. STATUS AND PROSPECTS FOR $\Delta\Sigma$ AND THE TOTAL OAM CONTRIBUTION

Similarly to what has been discussed in the previous section in connection with the gluon helicity density, the running integral of the quark singlet $\Delta\Sigma(x, Q^2)$ represents the intrinsic spin contribution of all quark flavors in the decomposition of the proton spin (2). Thanks to the direct coupling of the quarks to the probing virtual photon in DIS, $\Delta\Sigma(x, Q^2)$ is much better constrained by present fixed target data than the gluon helicity distribution which only enters indirectly through QCD scale evolution or as an $\mathcal{O}(\alpha_s)$ correction. Since $\Delta\Sigma(x, Q^2)$ and $\Delta g(x, Q^2)$ are coupled through the singlet evolution equations, any constraint from data on either of the two distribution impacts also the other one.

An extraction of the quark singlet from DIS data on $g_1(x, Q^2)$ also requires us to determine simultaneously two additional flavor nonsinglet distributions, which, if needed, can be all recast into the total contributions from u, d, and s quarks, i.e., $\Delta u + \Delta\bar{u}$, $\Delta d + \Delta\bar{d}$, and $\Delta s + \Delta\bar{s}$ (here we ignore for simplicity any contribution from charm and bottom quarks, which play no role for all currently available data).

The x-integrals of the two nonsinglet combinations are usually assumed to be related to the hyperon decay constants F and D within some uncertainties, which provide some indirect constraint for the currently unmeasured small x region below a few times 10^{-3}. Since we only wish to focus on the quark flavor singlet in this paper, we adopt these constraints in the same way as was done in the DSSV global analyses. A more thorough analysis of flavor

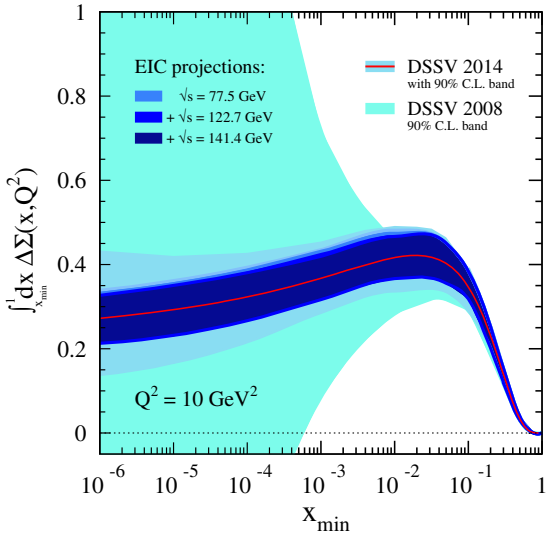

FIG. 7 (color online). Similar to Fig. 4 but now for the running integral of the quark singlet helicity density $\Delta\Sigma$. The solid line corresponds to the optimum fit of DSSV 2014 [17]. 90% C.L. uncertainty estimates (shaded bands) are shown for the DSSV 2008 and 2014 analyses and after including the different sets of projected EIC data.

separated quark helicity densities and their uncertainties will be conducted once a fully updated suite of reliable sets of fragmentation functions becomes available to revisit our previous impact study of SIDIS data in Ref. [8]. Then we will also explore how well an EIC can challenge the constraints imposed on the quark sector by the hyperon decays, one of which is related to the Bjorken sum rule, and the other, more important one mainly to the amount of strangeness polarization in the nucleon.

In Fig. 7 we show 90% C.L. estimates for the running integral of $\Delta\Sigma(x,Q^2)$ as a function of $x_{\min}$ for $Q^2 = 10\ \mathrm{GeV}^2$ for fits including different sets of existing and projected data. One should notice that the vertical axis here covers only half of the range shown for the running integral of Δg in Fig. 4. Also, $\Delta\Sigma(Q^2)$ enters the spin sum rule (2) with a factor of $1/2$ relative to the gluon spin contribution.

The outermost shaded band represents uncertainties as present in the original DSSV global analysis from 2008 [9]. They appear to be very significant for $x_{\min} \lesssim 10^{-3}$. As usual, the solid line shows the optimum fit of DSSV 2014 extrapolated down in x. The corresponding uncertainties are much reduced as compared to the 2008 analysis due to including additional DIS data from the COMPASS Collaboration and, indirectly, through constraints on Δg from RHIC pp data [15,16].

The set of three innermost shaded bands illustrates the significant impact of an EIC from a series of global fits that successively include the projected DIS data sets starting from the one corresponding to the lowest c.m.s. energy. The addition of the sets with increasing c.m.s. energy has less impact on the uncertainties than for the gluon helicity distribution shown in Fig. 4. For $x_{\min} = 10^{-6}$ and with an EIC, one expects from our studies to control the value of $\Delta\Sigma$ to within about 15% which is somewhat worse than what can be achieved for Δg. Also, the convergence of the running integral for $\Delta\Sigma$ for the DSSV 2014 best fit is much slower than for the gluon density shown in Fig. 4. This can be mainly attributed to the behavior of the strangeness helicity distribution that inclusive DIS data by themselves cannot constrain at all without imposing the above mentioned constraints on its first moment $\Delta s(Q^2) + \Delta\bar{s}(Q^2)$ from the hyperon decay constants F and D. Like in the DSSV analyses [9,10,17], the existing fixed-target SIDIS data used in our fit lead to a very small net strangeness polarization in the x range covered by data. The hyperon decay constants in turn demand a sizable negative total strangeness polarization which then has to be acquired somehow in the unmeasured small x region and, in our case, leads to the slow convergence of the quark singlet $\Delta\Sigma(Q^2)$. Only an EIC will be able to verify the validity of these assumptions by determining the x-shape of the sea quark distributions, in particular, $\Delta s(x,Q^2)$, down to unprecedentedly small values of x from a series of SIDIS measurements with identified pions and kaons. Once this is achieved, we expect that a future combined global analysis of SIDIS and DIS data will also lead to a much improved uncertainty estimate on the integral of $\Delta\Sigma$ compared to what is presented here.

As we have demonstrated in Figs. 4 and 7, an EIC will deliver a precise picture of the intrinsic spin contributions of quarks and gluons to within at least 10%–15% relative uncertainties. This information can be used along with the proton's spin decomposition (2) to estimate how much is left for the combined contribution $\mathcal{L}(Q^2)$ from the orbital motion of quarks and gluons. This is illustrated in terms of the running integral of $\mathcal{L}(Q^2)$ in Fig. 8 along with our usual set of uncertainty estimates based on the different sets of existing and projected experimental data.

The solid line gives the estimate for $\mathcal{L}(Q^2)$ for $Q^2 = 10\ \mathrm{GeV}^2$ based on extrapolating the best fit results of DSSV 2014 for $\Delta g(x,Q^2)$ and $\Delta\Sigma(x,Q^2)$ down to $x_{\min}$ and subtracting them off the total proton spin of $1/2$. As it turns out, at this particular value of Q^2, the DSSV 2014 result converges to basically a zero net contribution from OAM to the spin sum rule (2) but within huge uncertainties. The latter is given for both the DSSV 2008 and 2014 global fits by the outermost and middle shaded bands, respectively. As one can already anticipate from our studies performed in Figs. 4 and 7, an EIC will yield an excellent indirect constraint on $\mathcal{L}(Q^2)$ by combining the then available precise information on Δg and $\Delta\Sigma$. As can be inferred from the corresponding uncertainty estimates (set of innermost shaded bands), one can expect to constrain the net OAM contribution of quarks and gluons to within about ± 0.05 when all three sets of projected DIS data are combined. Of course, only a set of dedicated measurements

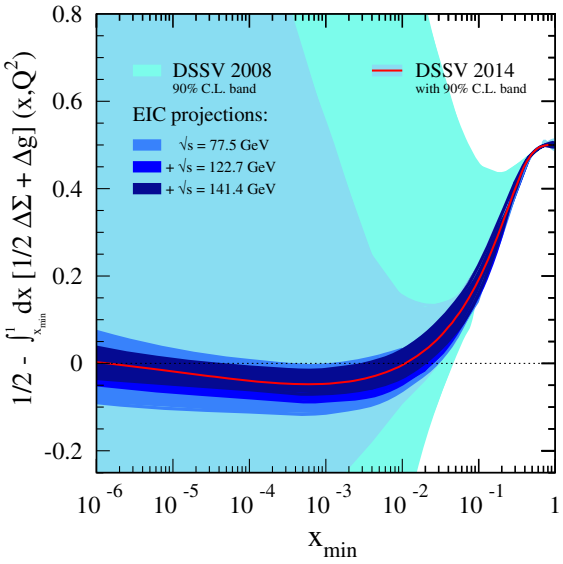

FIG. 8 (color online). As in Fig. 7 but now showing the contribution from the combined quark and gluon OAM $\mathcal{L}(Q^2)$ using Eq. (2) and the results obtained for the running integrals of Δg and $\Delta\Sigma$. As before, 90% C.L. uncertainty estimates (shaded bands) illustrate the impact of different projected EIC data sets.

at an EIC can reveal a detailed, hopefully flavor separated, quantitative picture of the orbital motion of quarks and gluons. For instance, even if the net OAM contribution turns out to be small as for the DSSV 2014 best fit, there might be significant cancellations among the individual quark flavors and the gluon. In addition, $\Delta g(Q^2)$ in (2) evolves logarithmically with Q^2 such that any increase has to be compensated by a corresponding decrease of $\mathcal{L}(Q^2)$, and vice versa, to always arrive at $1/2$. We recall that $\Delta\Sigma(Q^2)$ is a renormalization group invariant at LO and, in the $\overline{\text{MS}}$ scheme, evolves only very slowly with Q^2. However, separating quark and gluon OAM in Eq. (2) experimentally involves determinations of twist-3 generalized parton as well as quantum phase-space Wigner distributions which will be very challenging and still needs further theoretical work and perhaps lattice QCD studies; see, for instance, Refs. [7] and [35].

V. SUMMARY AND CONCLUSIONS

The electron-ion collider project constitutes a versatile and vast program to considerably deepen our knowledge of the inner workings of nucleons and nuclei and the underlying dynamics and interactions of quarks and gluons as governed by quantum chromodynamics. We have presented a detailed account of what can be achieved in the field of spin physics, in particular, the complex interplay of quark and gluon spins and their orbital motions yielding the known spin $1/2$ of the proton, for which we still lack a detailed quantitative understanding despite more than 30 years of intense research.

In the present study, we have considerably updated and refined our previous analysis on the impact of future EIC polarized DIS data in connection to our understanding of the gluon spin and its share in the proton spin budget. Throughout, we have explored the consequences of the much larger degree of gluon polarization in the nucleon than it has hitherto been acknowledged, as implied by the most recent RHIC results. In addition, we have used realistic projections for several forthcoming sets of RHIC data to estimate to what extent they further constrain the gluon helicity distribution by the end of the RHIC program. This baseline was used to quantify the expected impact of a future polarized DIS program at an EIC.

To this end, we have focused on providing accurate estimates of uncertainties for the running integrals as a function of the minimum momentum fraction for the gluon and quark singlet helicity distributions. Results were obtained in the context of global QCD analyses based on current and various projected sets of data and using the robust Lagrange multiplier technique for all error estimations. In case of the gluon helicity distribution we also provided detailed uncertainty studies bin by bin in momentum fractions to establish where the running integral receives major contributions and to determine below which value of x one can expect the integral to converge.

We find that the RHIC spin program still has quite some potential in reducing current uncertainties in the gluon helicity distribution by ruling out extreme variations in its shape. Nevertheless, one cannot expect to arrive at any meaningful and reliable estimate of the gluon contribution in the proton spin decomposition due to remaining substantial extrapolation uncertainties from the unmeasured region of small momentum fractions. Even under very conservative assumptions for its performance, an EIC with a sufficiently high enough center-of-mass system energy to reach deep into the so far unexplored kinematic regime will decisively constrain both the gluon and the singlet quark helicity densities and, at last, elevate the field of QCD spin physics into a precision era. For the corresponding x-integrals relevant for the proton's spin decomposition we expect to achieve relative uncertainties of about 10%. For the first time, this will also lead to a precise indirect estimate of the remaining contribution to the proton spin from the combined orbital motion of quarks and gluons, well before an EIC will be able to determine them directly. Estimates obtained by extrapolating our current best knowledge of helicity densities, without EIC data, to small momentum fractions point to a surprisingly small net orbital angular momentum in the proton's spin budget at intermediate scales Q^2, albeit within very large uncertainties. Of course, only an EIC can tell what the real value for the net orbital angular momentum actually is, and, if it indeed turns out to be small, how the contributions from the different quark flavors and the gluon conspire to yield that result.

ACKNOWLEDGMENTS

We are grateful to A. Bazilevsky and C. Gagliardi for providing us with the projections for the RHIC spin program. R. S. and M. S. are grateful to Brookhaven National Lab for hospitality while completing this study. This work was partially supported by CONICET, ANPCyT, UBACyT, the U.S. Department of Energy under Contract No. DE-SC0012704, and the Institutional Strategy of the University of Tübingen (DFG, ZUK 63).

[1] For a review of DIS fixed target data, see, e.g., C. A. Aidala, S. D. Bass, D. Hasch, and G. K. Mallot, Rev. Mod. Phys. **85**, 655 (2013).
[2] D. Boer *et al.*, arXiv:1108.1713.
[3] A. Accardi *et al.*, arXiv:1212.1701.
[4] E. C. Aschenauer *et al.*, arXiv:1409.1633.
[5] E. C. Aschenauer, S. Fazio, K. Kumericki, and D. Mueller, J. High Energy Phys. 09 (2013) 093.
[6] See, e.g., J. C. Collins, D. E. Soper, and G. F. Sterman, Adv. Ser. Dir. High Energy Phys. **5**, 1 (1989).
[7] E. Leader and C. Lorce, Phys. Rep. **541**, 163 (2014).
[8] E. C. Aschenauer, R. Sassot, and M. Stratmann, Phys. Rev. D **86**, 054020 (2012).
[9] D. de Florian, R. Sassot, M. Stratmann, and W. Vogelsang, Phys. Rev. Lett. **101**, 072001 (2008).
[10] D. de Florian, R. Sassot, M. Stratmann, and W. Vogelsang, Phys. Rev. D **80**, 034030 (2009).
[11] A. Adare *et al.* (PHENIX Collaboration), Phys. Rev. D **79**, 012003 (2009).
[12] A. Adare *et al.* (PHENIX Collaboration), Phys. Rev. Lett. **103**, 012003 (2009).
[13] L. Adamczyk *et al.* (STAR Collaboration), Phys. Rev. D **86**, 032006 (2012).
[14] L. Adamczyk *et al.* (STAR Collaboration), Phys. Rev. D **89**, 012001 (2014).
[15] L. Adamczyk *et al.* (STAR Collaboration), Phys. Rev. Lett. **115**, 092002 (2015).
[16] A. Adare *et al.* (PHENIX Collaboration), Phys. Rev. D **90**, 012007 (2014); **91**, 032001 (2015).
[17] D. de Florian, R. Sassot, M. Stratmann, and W. Vogelsang, Phys. Rev. Lett. **113**, 012001 (2014).
[18] E. R. Nocera *et al.* (NNPDF Collaboration), Nucl. Phys. **B887**, 276 (2014).
[19] B. Jager, A. Schafer, M. Stratmann, and W. Vogelsang, Phys. Rev. D **67**, 054005 (2003).
[20] B. Jager, M. Stratmann, and W. Vogelsang, Phys. Rev. D **70**, 034010 (2004).
[21] R. Sassot, in *5th International Workshop on Physics Opportunities at an Electron-Ion Collider (POETIC 2014)*, New Haven, CT, USA, 2014.
[22] E. C. Aschenauer *et al.* (RHIC Spin Collaboration), arXiv:1501.01220.
[23] See, e.g., *RHIC spin contributions to the 21st International Symposium on Spin Physics (SPIN 2014), Beijing, China, 2014 and to the XXIII International Workshop on Deep-Inelastic Scattering and Related Subjects (DIS 2015), Dallas, TX, USA, 2015* (World Scientific Publishing, 2015).
[24] D. Stump, J. Pumplin, R. Brock, D. Casey, J. Huston, J. Kalk, H. L. Lai, and W. K. Tung, Phys. Rev. D **65**, 014012 (2001).
[25] Recent global PDF fits can be found in R. D. Ball *et al.* (NNPDF Collaboration), J. High Energy Phys. 04 (2015) 040; L. A. Harland-Lang, A. D. Martin, P. Motylinski, and R. S. Thorne, Eur. Phys. J. C **75**, 204 (2015); S. Dulat *et al.*, arXiv:1506.07443.
[26] D. de Florian, R. Sassot, M. Epele, R. J. Hernández-Pinto, and M. Stratmann, Phys. Rev. D **91**, 014035 (2015).
[27] D. de Florian, R. Sassot, and M. Stratmann (to be published).
[28] E. C. Aschenauer, T. Burton, T. Martini, H. Spiesberger, and M. Stratmann, Phys. Rev. D **88**, 114025 (2013).
[29] See, e.g., D. de Florian and R. Sassot, Phys. Rev. D **51**, 6052 (1995).
[30] H. Abramowicz *et al.* (H1 and ZEUS Collaborations), arXiv:1506.06042.
[31] For the most recent DIS measurement, see C. Adolph *et al.* (COMPASS Collaboration), arXiv:1503.08935.
[32] R. Mertig and W. L. van Neerven, Z. Phys. C **70**, 637 (1996); W. Vogelsang, Phys. Rev. D **54**, 2023 (1996); S. Moch, J. A. M. Vermaseren, and A. Vogt, Nucl. Phys. **B889**, 351 (2014); Phys. Lett. B **748**, 432 (2015).
[33] R. D. Ball *et al.* (NNPDF Collaboration), Phys. Lett. B **728**, 524 (2014).
[34] S. J. Brodsky, M. Burkardt, and I. Schmidt, Nucl. Phys. **B441**, 197 (1995).
[35] See, e.g., C. Lorce, B. Pasquini, X. Xiong, and F. Yuan, Phys. Rev. D **85**, 114006 (2012); X. Ji, X. Xiong, and F. Yuan, Phys. Rev. Lett. **109**, 152005 (2012); Phys. Rev. D **88**, 014041 (2013); and references therein.